

# Machine-Learning-Driven Advanced Characterization of Battery Electrodes

Donal P. Finegan,<sup>†</sup> Isaac Squires,<sup>†</sup> Amir Dahari, Steve Kench, Katherine L. Jungjohann, and Samuel J. Cooper\*



Cite This: *ACS Energy Lett.* 2022, 7, 4368–4378



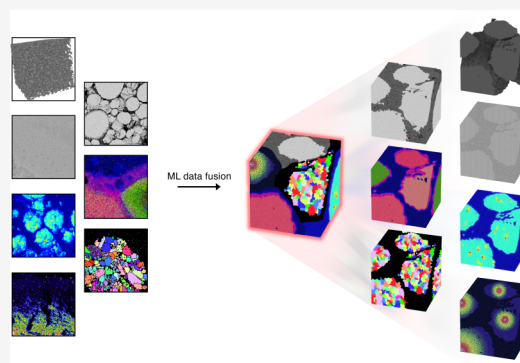
Read Online

ACCESS |

Metrics & More

Article Recommendations

**ABSTRACT:** Materials characterization is fundamental to our understanding of lithium ion battery electrodes and their performance limitations. Advances in laboratory-based characterization techniques have yielded powerful insights into the structure–function relationship of electrodes, yet there is still far to go. Further improvements rely, in part, on gaining a deeper understanding of complex physical heterogeneities in the materials. However, practical limitations in characterization techniques inhibit our ability to combine data directly. For example, some characterization techniques are destructive, thus preventing additional analyses on the same region. Fortunately, artificial intelligence (AI) has shown great potential for achieving representative, 3D, multi-modal datasets by leveraging data collected from a range of techniques. In this Perspective, we give an overview of recent advances in lab-based characterization techniques for Li-ion electrodes. We then discuss how AI methods can combine and enhance these techniques, leading to substantial acceleration in our understanding of electrodes.



“You cannot manage what you cannot measure” is an engineering adage to encourage measurement of parameters that can explain the success of a strategic change. This adage is also applicable in the field of lithium ion battery technology. The performance of Li-ion cells is linked to numerous material properties involving spatially and temporally varying chemistry, crystallography, and morphology. Managing these properties to achieve favorable cell performance has led to considerable improvements in Li-ion batteries since they were first commercialized. Often, management of material properties can only be confirmed by using advanced characterization techniques, yet there remains much that cannot be measured due to physical or practical limitations of analytical equipment.

Over the past decade, there has been tremendous progress in artificial intelligence (AI) techniques to enhance, merge, predict, classify, or artificially generate data.<sup>1–3</sup> This has coincided with materials characterization equipment achieving higher resolution than ever before, acquiring data in shorter times, and having streamlined multi-modal data processing routes. Numerous commercial data-analysis software packages have started to include AI techniques to, for example, enhance spatial resolution, correlate data across multi-modal techniques, or identify and quantify features within the data. Every year, new approaches of applying AI to further enhance data are demonstrated, many of which are seen in commercial

products not long after. A particularly relevant example is that, through the use of AI techniques, datasets are being generated with detail beyond what any single characterization technique can achieve, thus exceeding equipment limitations.

Despite the progress to date, there remains ample opportunity to apply AI techniques to further advance our characterization capabilities, thus empowering researchers to measure and therefore manage battery material properties that are otherwise unobtainable. In this Perspective, we provide an overview of the multi-length-scale battery material properties of interest, the limitations of lab-based materials characterization techniques, and the recent developments in AI that can be used to overcome these limitations. Our Perspective focuses on how generative adversarial networks (GANs) can be used in conjunction with multi-modal data to transcend systematic limitations of microscopy techniques. Finally, we will outline a view of the future where AI techniques enable the fusion of

Received: September 2, 2022

Accepted: October 28, 2022

Published: November 9, 2022



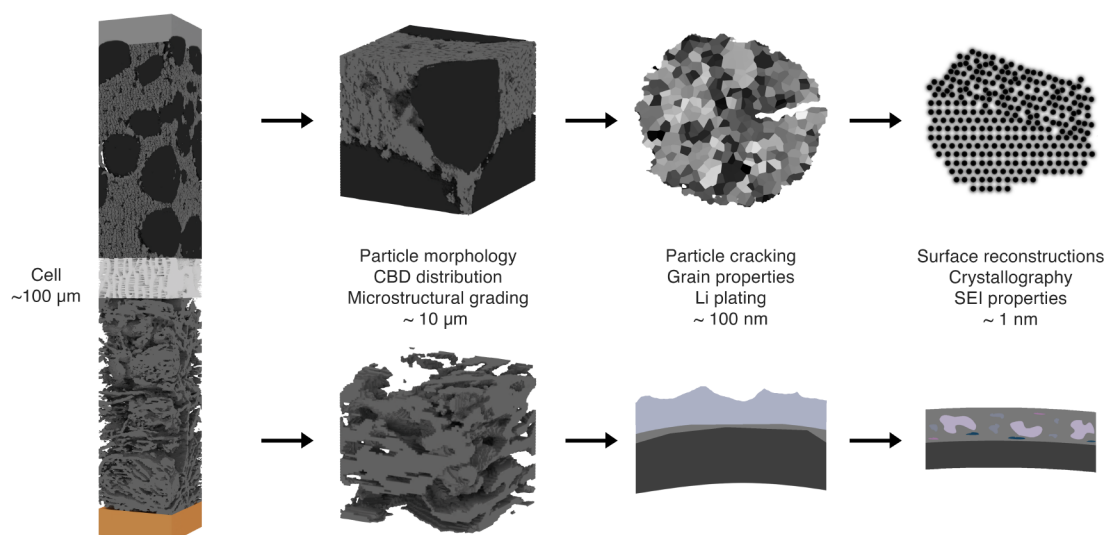


**Figure 1.** Illustration showing examples of multi-length-scale morphological, chemical, and crystallographic properties that influence the electrochemical behavior of electrodes throughout their cycle-life. 100  $\mu\text{m}$ : the full cell from top to bottom - aluminum current collector, NMC cathode, polymer separator, graphite anode, copper current collector. 10  $\mu\text{m}$ : top - in the cathode the gray phase is the carbon binder domain (CBD) and the black phase is the active material; bottom - in the anode the gray phase is graphite. 100 nm: top - an image of a single NMC crystal where the subparticle polycrystalline structure is visible; bottom - the growth of lithium plating on the surface of the active material, the light blue phase represents lithium, light gray the SEI and dark gray the active material. 1 nm: top - an atomic-scale image of a crystalline interface; bottom - a schematic of the composition of the SEI, which is commonly made up of various inorganic compounds.

data into a unified, multi-modal dataset that spans many length scales.

## 1. IMPORTANT PROPERTIES FOR ELECTRODE PERFORMANCE

There are a wide variety of electrode materials and electrolyte chemistries used in Li-ion batteries today. For simplicity, we focus our attention on conventional Li-ion cell materials with a graphite anode, a  $\text{LiNi}_x\text{Mn}_y\text{Co}_z\text{O}_2$  (NMC) cathode, a porous polymer separator, and a liquid electrolyte. Across the length scales from hundreds of micrometers down to nanometers, chemical, crystallographic, and morphological properties dictate the electrochemical performance of the cell throughout its cycle-life (Figure 1). Our understanding of these structure–function relationships is critical to defining operational limitations and degradation pathways, as well as identifying opportunities to improve the performance of cells.

Electrodes are typically around 100  $\mu\text{m}$  thick, and the geometry of their porous microstructure must achieve a delicate balance between ionic transport through the pores and electronic conduction through the solid. In addition, the volume fraction of the active material should be maximized, and enough active surface area should be available to facilitate homogeneous (de)lithiation. Manufacturers aim to achieve the highest energy density possible while still maintaining sufficient rate and life performance for a particular application. If the electrode is not porous enough or the pore network is too tortuous, there can be ion transport limitations at high operational rates, leading to concentration gradients, lithiation gradients, and reduced performance.<sup>4,5</sup>

As illustrated in Figure 1, morphological properties of the electrode, such as the pore size distribution and tortuosity factor, can influence the transport of Li ions from the separator to the current collector. A favorable distribution of conductive carbon and binder throughout a cathode is also important to achieve sufficient electrical conductivity.<sup>6,7</sup> Tuning manufactur-

ing conditions to optimize these electrode properties for specific applications can be accelerated with data from high-throughput characterization techniques able to quantify the key morphological metrics of the electrodes.

Across the length scales from hundreds of micrometers down to nanometers, chemical, crystallographic, and morphological properties dictate the electrochemical performance of the cell throughout its cycle-life.

At the particle level ( $\mu\text{m}$ -scale), characterizing properties relevant to Li transport requires inter- and intraparticle characterization. For example, the layered crystal structure of NMC facilitates transport of Li along the stacked planes of the crystal lattice. As such, the orientation of these planes relative to the particle surface will determine how, and in which directions, Li will intercalate into the particle. Therefore, not only is the morphology of the particle's outer surface important to characterize, but knowledge of the morphology and orientation of intraparticle crystals is needed for a complete understanding of Li transport, rate limitations, and opportunities for particle-level optimization. This is demonstrated by measured diffusion coefficients of polycrystalline NMC111,<sup>8</sup> NMC532,<sup>9,10</sup> and NMC811,<sup>11,12</sup> which differ by an order of magnitude across the literature.

Previous work has shown that grain size,<sup>13,14</sup> the density of grain boundaries,<sup>15</sup> and grain orientations<sup>16</sup> also significantly influence the rate capability and cycle life of NMC electrodes. Upon lithiation and delithiation, the crystal lattice of NMC displays anisotropic expansion and contraction that causes mechanical and crystallographic strain and subparticle cracking.<sup>17</sup> The propagation of cracks and how the dynamic crack growth is influenced by intraparticle architectures, and

Table 1. Examples of Multi-modal Lab-Based Techniques and Their Capabilities<sup>a</sup>

technique	typical best resolution	information	spatial ability	destructive?	environment requirement
TEM	~1 nm	morphology, atomic arrangement	2D	yes <sub>sp</sub>	—
EELS	~1 nm	bonding, chemical	2D	yes	—
APT <sup>28,29</sup>	~1 nm	chemical	3D	yes	vacuum
SPM/SSRM <sup>30,31</sup>	~1 nm	morphology, resistivity	2D	no	—
AFM	~1 nm	mechanical, morphology	2D	no	—
SEM †	~10 nm	morphology	2D	no*	vacuum
XCT <sup>32,33</sup>	~30 nm	morphology	3D	no or yes <sub>sp</sub>	—
EBSD <sup>27,34</sup> †	~50 nm	crystallographic	2D	no*	vacuum
EDS †	~100 nm	chemical	2D	no*	—
TOF-SIMS †	~1 μm	chemical	2D	yes	vacuum
DCT <sup>35</sup>	~100 μm	crystallographic	3D	no	—
(†) FIB sectioning	~10 nm	n/a	3D	*yes	vacuum

<sup>a</sup>The † symbol refers to the fact that many 2D imaging techniques can collect 3D information when used in combination with FIB serial sectioning. The \* symbol refers to the fact that any technique that uses FIB sectioning to generate 3D volumes becomes destructive. Subscript “sp” specifies that although the sample is not destroyed by the imaging itself, the sample preparation required before imaging will typically require destroying the component from which the sample was taken. Abbreviations: transmission electron microscopy (TEM), electron energy loss spectroscopy (EELS), atom probe tomography (APT), scanning probe microscopy (SPM), scanning spreading resistance microscopy (SSRM), atomic force microscopy (AFM), scanning electron microscopy (SEM), X-ray computed tomography (XCT), electron backscatter diffraction (EBSD), energy dispersive spectroscopy (EDS), time-of-flight secondary mass spectroscopy (TOF-SIMS), diffraction contrast tomography (DCT), and focused ion beam (FIB).

how cracks relate to performance loss, is also not well understood and requires advanced morphological characterization in 3D. Cracks bridge μm to nm length scales, where crack nucleation has been observed at the atomic scale<sup>17</sup> and cracks continue to grow until they are visible at the μm-scale. This makes cracks extremely challenging to characterize because multi-length-scale 3D imaging techniques are necessary to quantify their presence and create a direct link to the electrochemical function of the electrode. Li plating and dendrite growth also span length scales from nucleation of Li plating to growth of Li microstructures.

At the nm-scale, further structural, chemical, and morphological features exist that influence cell performance and cycle-life. For example, the surface of Ni-rich chemistries such as NMC811 undergo oxygen loss and consequent surface reconstruction to spinel or rock-salt structures during a cell's cycle-life.<sup>18,19</sup> This surface reconstruction can cause high interfacial lattice strain between the bulk layered NMC structure and its thin rock-salt surface that increases electrode impedance.<sup>20</sup> Surface treatments can also be intentionally applied to improve electrode performance, such as by creating composition or crystallographic gradients from the surface to the bulk of the particles to enhance stability and therefore the cycle-life of electrodes.<sup>21,22</sup> These surface effects are on the scale of nanometers, and their characterization is critical to understanding electrode degradation and validating methods to alter surface structures for enhanced cell performance. The solid electrolyte interphase (SEI) is also at the nm-scale and is a key contributor to the stability of the interface between the active material and electrolyte.

This list of multi-scale properties is not all-encompassing of performance-influencing factors, but it provides topical examples of why multi-scale characterization of morphology, chemistry, and crystallography within electrodes is critical to achieve an understanding of structure–function relationships. Such properties are also spatially heterogeneous across the length scales, the extent of which is expected to be highly influential on a cell's electrochemical behavior, highlighting the

need for high-resolution characterizations of representative 3D volumes.

## 2. CHARACTERIZATION ACROSS LENGTH SCALES AND LIMITS OF TECHNIQUES

Characterization of the morphological, crystallographic, and chemical properties across length scales is critical to understanding structure–function relationships for Li-ion electrodes. The selection and sequence of techniques to acquire this information is important but can be complex due to each technique having specific strengths and systematic limitations. While we acknowledge the tremendous progress and capabilities of synchrotron sources for multi-length scale and multi-modal characterization, here we focus on laboratory-based techniques that are more widely and readily accessible to the research community.

Table 1 gives an overview of frequently used lab-based techniques, their capabilities, and systematic limitations. Figure 2 shows some examples of techniques from Table 1 that were applied to Li-ion battery electrodes. To create a direct link between the material properties of electrodes and their electrochemical performance, information from several distinct techniques would be required from the same material sample. An ideal characterization tool would provide a high-dimensional dataset containing morphological, chemical, and crystallographic detail across length scales in space and over time. For example, such a dataset might consist of 3D coordinates of voxels where each voxel contains information on local material properties such as diffraction information, resistivity, mechanical properties, and chemical composition.

However, as Table 1 shows, there are systematic limitations that prevent the acquisition of multi-modal detail from the same sample. First, many techniques are destructive and so inherently prevent a sample from being imaged in a different system for correlative microscopy. Sample preparation is another considerable challenge for many techniques. Li-ion electrode samples are often air-sensitive, and preparing samples for imaging can be tedious and time-consuming. For example,



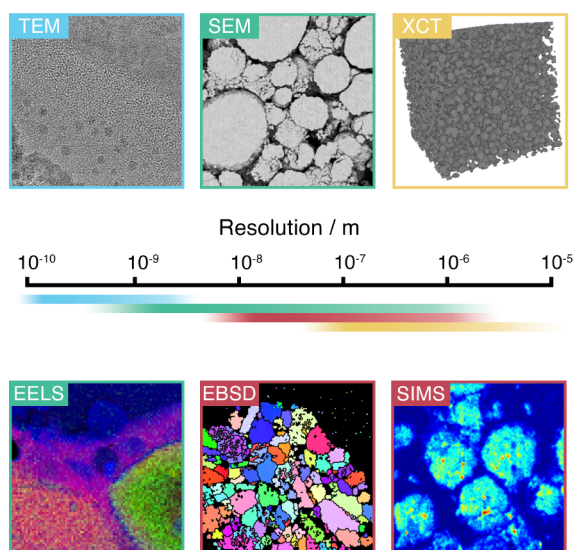


**Figure 2.** Examples of recent morphological, structural, and chemical characterization achievements across the length scales for Li-ion electrodes. References for adapted images are as follows: EELS,<sup>23</sup> SIMS,<sup>24</sup> TEM,<sup>25</sup> SEM,<sup>26</sup> and EBSD.<sup>27</sup> The resolution scale is indicative of typical practice found in the literature today.

TEM methods require samples to be thin enough for electrons to pass through them (typically less than 100 nm, or less than 10 nm for atomic resolution), followed by micro-manipulation of the sample slice for mounting and imaging. Another example of a limitation caused by sample preparation is how nano-XCT requires samples that are not much wider than the field of view (around 0.1 mm) for optimal attenuation. The challenges facing sample preparation can render the technique infeasible for gaining statistical confidence or make it impossible to do correlative metrology using multiple techniques and length scales. Progress is being made, and with the recent introduction of laser milling in electron microscopes, the time needed for cutting small samples has been considerably reduced,<sup>36</sup> but the challenges still remain.

There are systematic limitations that prevent the acquisition of multi-modal detail from the same sample.

The limitations of the characterization techniques have led to some interest in methods for blending multi-modal data-streams into a single dataset, where the strengths of each mode of imaging are leveraged to generate a new representative dataset with detail beyond that of each technique alone.<sup>37</sup> An example of this is work by Furat et al.,<sup>38</sup> where it was recognized that nano-XCT was excellent in capturing Li-ion electrode particle morphologies but lacked the ability to determine sub-particle crystallographic detail, while EBSD was excellent in recording sub-particle crystal detail but lacked the ability to capture full particle morphologies. Detail from the two data-streams were quantified, and a new representative dataset containing 3D crystallographic and particle morphological detail was generated. This work demonstrated the potential for merging distinct data-streams to generate more comprehensive data than any single technique could achieve alone. Xu et al.<sup>39</sup> used a similar approach of stochastic reconstruction to create an artificial but representative

architecture of a polymer separator material using input data from nano-XCT data and higher resolution 2D SEM data. While stochastic techniques have been shown to be effective, they are complex to build, and tend to be specifically designed for a particular material, rather than being generally applicable. As such, we are especially interested in the new family of machine learning (ML) techniques that can achieve greater breadth of application, with comparatively little expert fine-tuning required. For example, Dahari et al.<sup>40</sup> used data from distinct but complementary imaging techniques (XCT and SEM) to train deep convolution generative adversarial networks (GANs) to generate representative 3D images with multi-modal details. The opportunities to expand beyond this work to create high-dimensional data fusion and super-resolution datasets will be discussed in the following section.

### 3. MACHINE LEARNING METHODS FOR ENABLING NEXT-GENERATION MATERIALS CHARACTERIZATION

The rapid advancement of ML algorithms, along with continued improvement of computational power, has begun a paradigm shift in the approach to materials design, discovery, optimization, and characterization. Of particular interest is the wealth of existing computer vision research for image-based tasks, some of which can be applied to Li-ion microstructural datasets. Central to many of these approaches are convolutional neural networks (CNNs), which employ a neural network architecture designed to process image data inspired by biomimicry of the human visual system. CNNs have been key to image classification, but they also form the basis of many of the pioneering methods in object detection, image augmentation, and image generation. These ML methods have already helped to mitigate some of the limitations of the characterization techniques described above,<sup>45–47</sup> such as enhancing resolution and automating segmentation of structural features from images, and we believe that there is huge potential for further advances in the near future.

In many cases, established ML methods can be directly applied to materials characterization challenges. Examples of six of these scenarios are described below and also summarized in Figure 3.

**Segmentation**, the process of assigning each pixel/voxel a phase label, is an excellent example of a common materials science task that can be greatly aided by the appropriate use of AI. In a broader context, semantic classification of objects within images is important for a wide range of applications. A number of the advances in ML segmentation have come from the self-driving car research community, where recognizing and labeling objects within images is critical for the safety of passengers and pedestrians. CNNs have been very successful at semantic segmentation. “Encoder–decoder” architectures (CCNs with a bottleneck shape), such as U-Net,<sup>48</sup> have demonstrated high accuracy with short evaluation and training times, even with limited data.

In materials science, semantic segmentation is required before quantitative characterization or simulations are performed. “Thresholding” is a common segmentation method in the literature, where pixels are assigned to classes based only on their grayscale values relative to a fixed cutoff. However, thresholding has shown to have a high variability and poor performance at the boundary between different materials, which leads to misleading analysis of battery electrode microstructural images and, as such, should be avoided. As

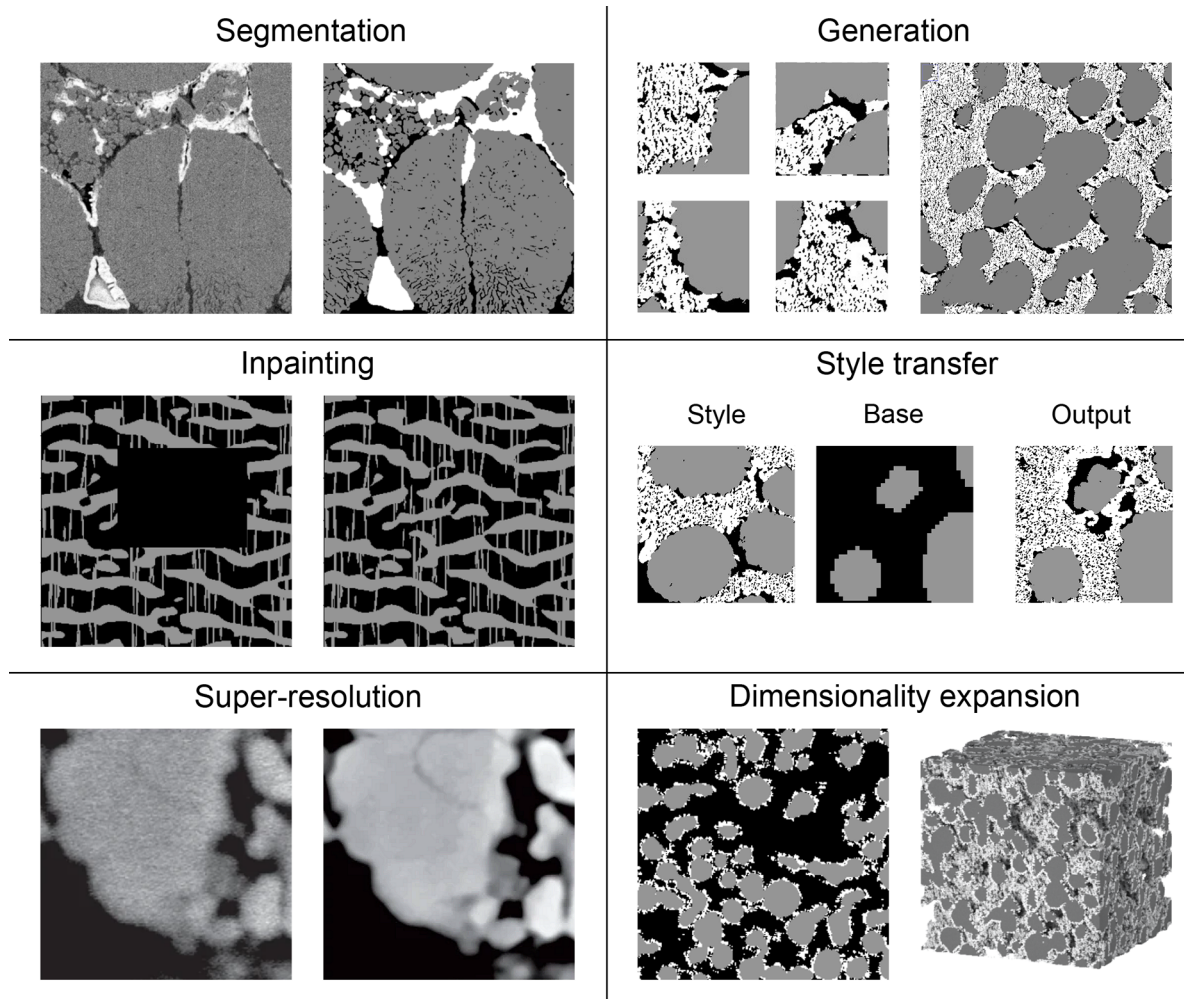


Figure 3. Examples of machine learning methods for enabling next-generation materials characterization. In each example, the image on the left shows the input, and the image on the right shows the output after the specified method was applied. In each case, the images were generated based on the approaches described in relevant studies: segmentation,<sup>26</sup> generation,<sup>41</sup> inpainting,<sup>42</sup> style transfer,<sup>40</sup> super-resolution,<sup>43</sup> and dimensionality expansion.<sup>44</sup>

outlined in sections 1 and 2, quantifying multi-length-scale morphological features from images is extremely important for creating structure–function relationships of battery materials. Quantification of morphological information almost always involves segmentation of gray scale images. CNN methods that improve the accuracy of segmentation and therefore of quantified morphological properties are expected to considerably improve our characterization capability in this space.

Trainable Weka Segmentation (TWS) is a ML approach which is available as a plug-in to ImageJ.<sup>49</sup> TWS provides the user with various ML frameworks for the classification of pixels, including neural networks, with the labeled training data input by the user via a graphical user interface. There are cases when the segmentation of phases is not clear with a single imaging technique. The input to a ML segmentation tool could be extended to include multi-modal data streams, as is demonstrated in the paper by Cooper et al. when complementary SEM images (secondary and backscattered electrons) of a battery cathode are used for segmentation.<sup>26</sup> Currently, the segmentation methods used in other domains such as autonomous vehicles are much more sophisticated, leaving significant scope for the introduction of these methods

into materials science workflows to improve the speed and accuracy of segmentation.

**Style transfer** is another common ML technique that can be applied to materials science. This method generates a dataset that adopts the appearance or stylistic details of a second dataset, while maintaining the structural features of the original data. Style transfer has been applied to a range of tasks, including modifying artwork to adopt the painting style of another painter.<sup>50</sup> As outlined in the previous sections, different imaging techniques provide different resolution, fidelity, and information. Consider two complementary techniques that capture different material properties, such as XCT and EBSD. A theoretical style transfer workflow could start with an XCT image, which captures the microstructural distribution of phases. A style transfer algorithm can be trained on EBSD data to understand the relationship between gross particle morphology and grain structure. This EBSD “style” can then be applied to the XCT image, resulting in microstructural volume, which includes subparticle crystallographic information. Employing style transfer could enable the fusion of different imaging techniques, yielding a pathway to beyond lab capability characterization for multi-modal datasets.

Missing or corrupted regions of an image can be filled in with a technique called **inpainting**. Deep convolutional models, particularly GANs and autoencoders, have been very successful at inpainting and have demonstrated their effectiveness in a range of applications of image reconstruction.<sup>51</sup> Many materials characterization techniques contain artifacts or corrupted regions. Broadly, there have been two approaches to inpainting in materials science. First, using classical statistical reconstruction methods such as exemplar-based inpainting, of which the most famous example is the PatchMatch algorithm.<sup>52</sup> Second, ML-based methods are starting to emerge which use GANs and autoencoders to detect and inpaint damaged regions.<sup>42,53,54</sup> It is important to note that stochastic inpainting methods do not aim to reconstruct the ground truth missing data exactly. Instead, the missing data is replaced with statistically similar generated data with matching boundaries. Inpainting enables the transformation of low-quality datasets into high-quality datasets, potentially avoiding repeating experiments and removing unwanted imaging artifacts. For example, low-quality high-resolution datasets are commonly collected from battery electrodes, as these materials are very sensitive to the electron beam used in TEM, EDS, and EELS, and therefore decreased collection intervals on the electrodes generate noisy datasets.<sup>55</sup> Although some ML techniques already exist, further exploitation of cutting edge ML research is possible to improve the quality of the inpainting, and more work is required to integrate these tools into existing workflows and make them more widely accessible to the community.

The rapid advancement of machine learning algorithms, along with continued improvement of computational power, has begun a paradigm shift in the approach to materials design, discovery, optimization, and characterization.

There are a multitude of ML data **generation** techniques, but the two most widely adopted are GANs and diffusion models. GANs are a family of generative ML models characterized by the use of two networks competing in an adversarial game eventually resolving in a network that can produce samples that mimic the underlying probability distribution of a training dataset.<sup>56</sup> Diffusion models are networks that learn to invert the process of adding Gaussian noise to an image.<sup>57</sup> Both methods have been very successful in generating complex fictitious data.<sup>58,59</sup> These methods can also be applied to data augmentation tasks where data availability is limited. This makes them a powerful tool in materials science, where collecting large field-of-view images of a macro-homogeneous materials is time-consuming and expensive. To this end, Gayon-Lombardo et al. demonstrated the ability of GANs to generate numerous arbitrarily large volumes of 3D microstructure (including battery materials) after training on a comparatively small volume of training data, with training algorithms similar to those used for conventional GANs.<sup>41</sup> These methods allow for the generation of datasets with physical extents beyond lab capabilities.

More recently, bespoke solutions to specific characterization challenges have been developed. 2D images can typically offer

higher resolution and better phase identification than their 3D CT-derived counterparts, while also often being faster and easier to obtain. However, many metrics of interest are inherently volumetric. For example, extracting the transport efficiencies (or tortuosity factors) of porous media requires a 3D volume of material. **Dimensionality expansion** is the process of using a lower-dimensional dataset to generate a higher-dimensional version. *SliceGAN* is a GAN-based method for dimensionality expansion proposed by Kench and Cooper.<sup>44</sup> This method uses homogeneous 2D microstructural training data to train a GAN that outputs 3D volumes of microstructure. The approach allows for the non-destructive generation of 3D datasets, providing the opportunity to perform comparative studies. This method also provides an opportunity to generate 3D datasets that were previously unobtainable if applied to a 2D imaging technique that has no 3D analogue. For example, EELS datasets are rich in chemical information at sub-nanometer resolution in 2D datasets but would require dimensionality expansion to observe nanometric chemical distributions in 3D volumes.

**Super-resolution** (SR) is the generation of a high-resolution image from a low-resolution image. There are many possible approaches to SR, with deep learning among the most effective. Super-resolution methods are useful when low-res imaging is cheaper, easier, or faster, or where the high-res image is difficult to obtain. There have been great advances in deep learning SR, most notably, for the application of facial recognition by super-resolving low-res faces taken in the natural environment. These ML-based methods employ CNNs with a range of architectures from GANs<sup>40,60</sup> to deep residual nets.<sup>61</sup> It is important to note the difference between super-resolution and super-sampling in the context of imaging for electrode characterization. Super-sampling generates new points in between those collected experimentally, therefore reducing the apparent step size while retaining the same field-of-view, whereas super-resolution is the improved capacity to distinguish between neighboring regions and can, in this context, be thought of as deblurring. Low-res data is more easily obtained, and therefore training a super-resolution model with a small set of high-res data could provide a shortcut to collecting representative volumes of high-res data. For example, consider an SEM micrograph of a cathode particle super-resolved with sub-10-nm features of the SEI from TEM data. As outlined in sections 2 and 3, bridging length scales remains a challenge for hardware and super-resolution presents tremendous opportunity for overcoming the continuous struggle between resolution and field of view in lab-based systems.

Validating methods that produce synthetic data is challenging when no ground truth experimental reference exists. This is the case for many of the ML tools outlined in this section. Assessing the quality of synthetic data by comparing various microstructural metrics you have not constrained during training to the ground truth is a useful validation technique, as this can assert whether your generated data has retained some of the implicit statistics of the dataset. Therefore, when developing these techniques, validation must first be explored in studies where the ground truth is available, before extending to cases where there is no ground truth.

As new techniques and methods are developed and adapted to solve materials characterization challenges, it is important to identify new assumptions that can be built into and enforced by AI algorithms. For example, when generating micro-



structural datasets, it is possible to encourage a GAN to produce the correct volume fractions of each material phase using an extra loss function term. This both simplifies the task of generation and can result in more accurate synthetic data. The SliceGAN algorithm demonstrates this by incorporating the assumptions of spatial homogeneity and isotropy.<sup>44</sup> This can vastly reduce computational expense as far fewer filters can be used compared to typical GAN generating structured images, such as faces, where different regions of the output must contain particular features. Thus, while it is exciting to try and make use of the most recent advances from the ML community, well thought through adaptations for materials science applications are crucial to fast progress in this field.

Our Perspective mainly discusses the application of GANs to materials characterization problems. This is due to the recent wave of success of GANs in this field, although they are not without their weaknesses and many efforts have been made to characterize their failure modes.<sup>62</sup> Notoriously, they suffer from instability during training and commonly get stuck generating a small subset of possible outcomes (mode collapse). A study by the authors applied SliceGAN to a wide range of materials with a variety of feature complexities.<sup>63</sup> The model performed consistently well, indicating that these general GAN failure modes can be suppressed when solving general micrograph generation problems.

ML has the potential to help overcome many of the limitations of existing characterization techniques. The methods outlined in this section are already a useful set of tools, but they could be even more powerful when combined, as we now discuss.

#### 4. OPTIMIZATION AND DATA FUSION: ENVISAGING A FUTURE FOR AI AND MULTI-MODAL CHARACTERIZATION

The AI-powered enhancements to conventional characterization techniques described in the previous section will enable significant acceleration in understanding battery materials as they currently are; however, the exciting next step is to explore the consequences of combining them.

A powerful potential application of AI is the **optimization** of electrode morphology (microstructure, mesostructure, and cell geometry), which would lead to increases in energy density and reduced charge times by minimizing the losses resulting from the various electrochemical processes. In homogenized models, such as the Doyle–Fuller–Newman model,<sup>64</sup> the morphological properties are captured by parameters that can generally be trivially optimized in isolation. For example, tortuosity factors and particle radii should be minimized, while surface areas should be maximized. However, this is typically not an instructive exercise, as the resulting electrode properties are unlikely to be manufacturable, but even if they were, determining the appropriate processing conditions to obtain such a microstructure presents a significant challenge. As such, in order to be useful, morphological optimization needs to be linked to relevant manufacturing parameters.

Implementing these constraints presents an intimidating new challenge. One approach to address this problem is to use physics-based simulations to directly model the manufacturing processes and thus recover the space of possible electrodes.<sup>65</sup> However, this is computationally expensive and, in terms of complexity and validation, is a problem at least as difficult as battery modeling itself, unless highly simplified systems are used. While physics-based models may not be practical for

optimization of complex manufacturing conditions and supply chains, we note that they have tremendous utility for understanding the influence and optimization of specific material properties on cell performance.<sup>66</sup>

ML can offer data-driven methods that avoid the cost and complexity of direct simulation. The ability of GANs to learn to generate instances from implicit distributions describing complex systems based only on training examples is well aligned with this challenge. In particular, conditional GANs can learn to generate families of samples that correspond to a set of specified parameters,<sup>67</sup> which in this context could be manufacturing parameters. This means the relationship between manufacturing parameters and microstructural features could be learned using only information about the inputs (e.g., calendaring pressures or mass fractions) and the resulting outputs (e.g., microstructural image data).

AI-enhanced characterization can bridge systematic limitations that prevent the simultaneous collection of the numerous performance-influencing material properties.

Although a conditional GAN enables fast generation of novel microstructures, this does involve interpolating in the parameter space and generating previously unseen examples. The interpolation procedure is based on implicit relationships between the labels and the data, and not any physics-based relationships. This is a potential weakness of a GAN-based approach, and care must be taken to validate any interpolated results. Additionally, training such a conditional GAN would require careful collection of microstructural data with fixed manufacturing parameters. This is by no means trivial, and any issues in the data will be reflected in the output of the GANs. Although GANs are promising candidates, it is important that other methods for high-throughput, data-driven optimization of manufacturing parameters are explored.

Once a GAN's generator has been trained, it is very cheap to evaluate (i.e., to generate microstructural data), and metrics such as the tortuosity factor can also be cheaply extracted using open-source software such as *TauFactor*.<sup>68</sup> As such, conventional optimization approaches, such as Bayesian optimization, can then be applied to explore the manufacturing parameter space and predict optimal values for a particular application. In addition, this approach could also be adapted to intelligently suggest the next best cell to build and test in reality, based on both its expectation of high performance and its awareness of uncertainty.

Furthermore, the AI-enhanced characterization methods described in the previous section can be used to minimize the cost and difficulty of building the training set—for example, only requiring 2D information when using dimensionality expansion, or coping with hard-to-avoid experimental artifacts through inpainting.

Aside from optimization, the ML methods described in the previous section also offer a new approach for obtaining multi-modal datasets through **data fusion**, as was recently explored by Dahari et al.<sup>40</sup> As an example workflow, starting from a high-resolution SEM image, segmentation could first be used to generate a phase map. Dimensionality expansion can then be applied to generate a large 3D volume. Using this as a base

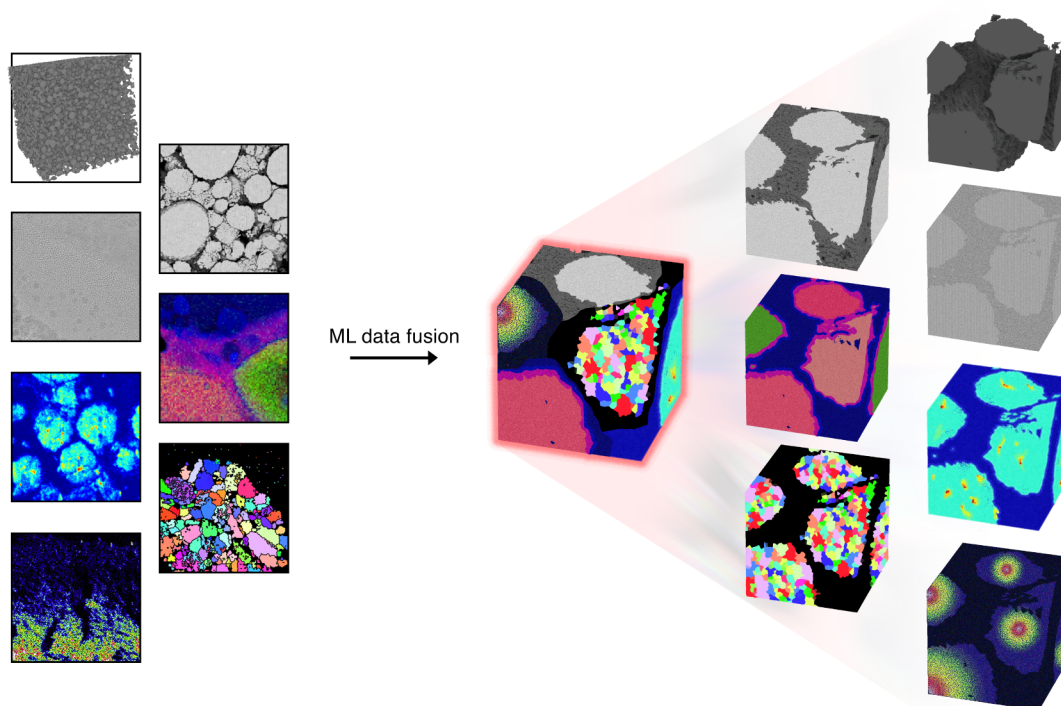


**Figure 4.** An imagined future workflow for data fusion using machine learning techniques. A range of characterization datasets are combined through machine learning techniques, resulting in a unified, multi-length-scale, and multi-modal dataset.

volume, style transfer and super-resolution methods could be used to project features from other characterization techniques onto each of the phases. A single voxel in the resulting dataset could thus contain a variety of properties, including chemical, crystallographic, electronic, mechanical, and many more.

Correlations between different properties could also be enforced, for example by applying different characterization techniques to the same region of a microstructure, extracting statistical relationships between them, and including this in the eventual loss during the style transfer process. Alternatively, correlations could be enforced using our understanding of the covariance between channels. For example, a resistivity map might show high diffusion coefficients at grain boundaries, which can subsequently be matched to the grain boundaries of EBSD data. While it is currently impossible to obtain a multi-modal 3D dataset using only characterization techniques, this approach could allow us to capture some of the key relationships between different physical properties. It would also allow different groups working on separate projects to unify their characterization results into a powerful dataset for multi-physics modeling, with the aim of unlocking new information about battery behavior.

The fusion of multi-modal datasets into a unified representation of battery electrodes (as illustrated in Figure 4) is a very appealing prospect, especially for characterization and modeling purposes. This alone would solve numerous challenges outlined in sections 2 and 3. However, there is also an opportunity to leverage AI techniques to change the historic paradigms of design and optimization of battery materials. Neural networks do not rely on human-readable or human-interpretable datasets. Constraining our networks to output data in forms such as 3D volumes representing different material properties so that we can model physical processes on them does not exploit the full power of data-driven ML. If

instead the imaging data was combined with other data-streams, then more abstract models could be built which use data from the end-to-end process, from fabrication to death. These models would bypass assumptions and simplifications baked into models or the constraints required to output human-readable results. Instead, this Deep Design approach would be fully data-driven, allowing us to see new relationships and ask new types of questions. To work toward this goal, considerable thought and planning is needed on relevant variables and the collection, organization, and processing of data.<sup>69</sup>

The performance of Li-ion batteries is determined by a plethora of constituent material properties across multiple length scales. This makes the task of creating a quantitative link between structure and function for Li-ion battery materials extremely challenging, requiring multi-modal and multi-length-scale datasets. To model and quantify the influence of specific material properties on battery performance without any assumptions requires a complete detailed spatial description of all influencing material properties, which is currently not achievable due to systematic limitations of the various characterization techniques.

AI-enhanced characterization can bridge systematic limitations that prevent the simultaneous collection of the numerous performance-influencing material properties. CNN-based methods in particular can enable the generation of higher resolution and higher dimensionality datasets than is otherwise experimentally achievable. Furthermore, data from all characterization techniques can be used to generate unified representative volumes of electrode microstructure. These unified volumes, in combination with electrochemical data, can enable detailed multi-physics simulations and high-throughput optimization. While a specific case example of Li-ion electrodes was used throughout this Perspective, the general approach is



widely applicable to other areas of energy materials research. These capabilities present a new paradigm for characterization, and high-quality data will be critical to its success.

## ■ ASSOCIATED CONTENT

### Data Availability Statement

No code was created with the content of this manuscript.

## ■ AUTHOR INFORMATION

### Corresponding Author

**Samuel J. Cooper** – Dyson School of Design Engineering, Imperial College London, London SW7 2DB, U.K.; Email: [samuel.cooper@imperial.ac.uk](mailto:samuel.cooper@imperial.ac.uk)

### Authors

**Donal P. Finegan** – National Renewable Energy Laboratory, Golden, Colorado 80401, United States; [orcid.org/0000-0003-4633-560X](https://orcid.org/0000-0003-4633-560X)

**Isaac Squires** – Dyson School of Design Engineering, Imperial College London, London SW7 2DB, U.K.

**Amir Dahari** – Dyson School of Design Engineering, Imperial College London, London SW7 2DB, U.K.

**Steve Kench** – Dyson School of Design Engineering, Imperial College London, London SW7 2DB, U.K.; [orcid.org/0000-0002-7263-6724](https://orcid.org/0000-0002-7263-6724)

**Katherine L. Jungjohann** – National Renewable Energy Laboratory, Golden, Colorado 80401, United States; [orcid.org/0000-0002-8132-1230](https://orcid.org/0000-0002-8132-1230)

Complete contact information is available at:

<https://pubs.acs.org/10.1021/acseenergylett.2c01996>

### Author Contributions

<sup>†</sup>D.P.F. and I.S. contributed equally.

### Notes

The authors declare no competing financial interest.

### Biographies

**Donal P. Finegan** is a senior scientist at the National Renewable Energy Laboratory (NREL). He leads NREL's X-ray computed tomography laboratory and Li-ion battery characterization group. His research focuses on understanding failure and degradation mechanisms of Li-ion batteries and ways to improve their safety and performance.

**Isaac Squires** is a Ph.D. student in the Dyson School of Design Engineering at Imperial College London. He is supervised by Dr. Samuel J. Cooper, and his research focuses on machine-learning-driven characterization and optimization of battery materials, alongside electrochemical modeling of Li-ion batteries.

**Amir Dahari** is a Ph.D. student in the Dyson School of Design Engineering at Imperial College London. He is supervised by Dr. Samuel J. Cooper and Dr. Dario Paccagnan. His research focuses on image data fusion techniques for battery materials characterization, alongside modeling of future mobility systems.

**Steve Kench** is a Ph.D. student in the Dyson School of Design Engineering at Imperial College London. His supervisor is Dr. Samuel J. Cooper, and his research focus is material characterization and optimization using machine-learning methods.

**Katherine Jungjohann** is a group manager for the Analytical Microscopy and Imaging Science group at NREL. Her research investigates in situ and cryogenic electron microscopy characterization of battery electrode/electrolyte interfaces, with an emphasis on high-rate cycled Li-metal anodes.

**Samuel J. Cooper** is an associate professor in the Dyson School of Design Engineering at Imperial College London. He is the leader of the Tools for Learning, Design, and Research (tldr) group. Sam is also passionate about online education and public communication of science. [tldr-group.github.io](http://tldr-group.github.io)

## ■ ACKNOWLEDGMENTS

D.P.F. was supported by the Alliance for Sustainable Energy, LLC, the manager and operator of the National Renewable Energy Laboratory for the U.S. Department of Energy (DOE) under contract number DE-AC36-08GO28308. Funding was provided by the U.S. Department of Energy Vehicle Technology Office. S.J.C. and S.K. were supported by funding from the EPSRC Faraday Institution Multi-Scale Modelling project (<https://faraday.ac.uk/>; EP/S003053/1, grant number FIRG003 received by A.D., S.K., and S.J.C.), and funding from the President's PhD Scholarships received by A.D. Funding from the Henry Royce Institute's Materials 4.0 initiative was also received by A.D. and S.J.C. (EP/W032279/1). Thanks to Daisy Thornton for providing valuable feedback on a draft of this manuscript.

## ■ REFERENCES

- (1) Scharf, J.; Chouchane, M.; Finegan, D. P.; Lu, B.; Redquest, C.; Kim, M.-c.; Yao, W.; Franco, A. A.; Gostovic, D.; Liu, Z.; Riccio, M.; Zelenka, F.; Doux, J.-M.; Meng, Y. S. Bridging nano- and microscale x-ray tomography for battery research by leveraging artificial intelligence. *Nat. Nanotechnol.* **2022**, *17* (5), 446–459.
- (2) Lombardo, T.; Duquesnoy, M.; El-Bouysidy, H.; Aren, F.; Gallo-Bueno, A.; Jørgensen, P. B.; Bhowmik, A.; Demortiere, A.; Ayerbe, E.; Alcaide, F.; Reynaud, M.; Carrasco, J.; Grimaud, A.; Zhang, C.; Vegge, T.; Johansson, P.; Franco, A. A. Artificial intelligence applied to battery research: Hype or reality? *Chem. Rev.* **2022**, *122* (12), 10899–10969.
- (3) Xu, H.; Zhu, J.; Finegan, D. P.; Zhao, H.; Lu, X.; Li, W.; Hoffman, N.; Bertel, A.; Shearing, P.; Bazant, M. Z. Guiding the design of heterogeneous electrode microstructures for li-ion batteries: Microscopic imaging, predictive modeling, and machine learning. *Adv. Energy Mater.* **2021**, *11* (19), 2003908.
- (4) Finegan, D. P.; Quinn, A.; Wragg, D. S.; Colclasure, A. M.; Lu, X.; Tan, C.; Heenan, T. M. M.; Jervis, R.; Brett, D. J. L.; Das, S.; Gao, T.; Cogswell, D. A.; Bazant, M. Z.; Di Michiel, M.; Checchia, S.; Shearing, P. R.; Smith, K. Spatial dynamics of lithiation and lithium plating during high-rate operation of graphite electrodes. *Energy Environ. Sci.* **2020**, *13*, 2570–2584.
- (5) Okasinski, J. S.; Shkrob, I. A.; Rodrigues, M.-T. F.; Raj, A.; Prado, A. Y. R.; Chuang, A. C.; Pidaparthi, S. S.; Abraham, D. P. Time-resolved x-ray operando observations of lithiation gradients across the cathode matrix and individual oxide particles during fast cycling of a li-ion cell. *J. Electrochem. Soc.* **2021**, *168* (11), 110555.
- (6) Chouchane, M.; Rucci, A.; Lombardo, T.; Ngandjong, A. C.; Franco, A. A. Lithium ion battery electrodes predicted from manufacturing simulations: Assessing the impact of the carbon-binder spatial location on the electrochemical performance. *J. Power Sources* **2019**, *444*, 227285.
- (7) Hein, S.; Danner, T.; Westhoff, D.; Prifling, B.; Scurtu, R.; Kremer, L.; Hoffmann, A.; Hilger, A.; Osenberg, M.; Manke, I.; Wohlfahrt-Mehrens, M.; Schmidt, V.; Latz, A. Influence of conductive additives and binder on the impedance of lithium-ion battery electrodes: Effect of morphology. *J. Electrochem. Soc.* **2020**, *167* (1), 013546.
- (8) Chouchane, M.; Primo, E. N.; Franco, A. A. Mesoscale effects in the extraction of the solid-state lithium diffusion coefficient values of battery active materials: Physical insights from 3d modeling. *J. Phys. Chem. Lett.* **2020**, *11* (7), 2775–2780.

- (9) Wang, C.; Yu, R.; Hwang, S.; Liang, J.; Li, X.; Zhao, C.; Sun, Y.; Wang, J.; Holmes, N.; Li, R.; Huang, H.; Zhao, S.; Zhang, L.; Lu, S.; Su, D.; Sun, X. Single crystal cathodes enabling high-performance all-solid-state lithium-ion batteries. *Energy Storage Materials* **2020**, *30*, 98–103.
- (10) Noh, H.-J.; Youn, S.; Yoon, C. S.; Sun, Y.-K. Comparison of the structural and electrochemical properties of layered  $\text{Li}[\text{Ni}_x\text{Co}_{1-x}\text{Mn}_2]\text{O}_2$  ( $x = 1/3, 0.5, 0.6, 0.7, 0.8$  and  $0.85$ ) cathode material for lithium-ion batteries. *J. Power Sources* **2013**, *233*, 121–130.
- (11) Ghosh, A.; Foster, J. M.; Offer, G.; Marinescu, M. A shrinking-core model for the degradation of high-nickel cathodes (nmc811) in li-ion batteries: Passivation layer growth and oxygen evolution. *J. Electrochem. Soc.* **2021**, *168* (2), 020509.
- (12) Sturm, J.; Rheinfeld, A.; Zilberman, I.; Spingler, F.B.; Kosch, S.; Frie, F.; Jossen, A. Spingler, Stephan Kosch, Fabian Frie, and Andreas Jossen. Modeling and simulation of inhomogeneities in a 18650 nickel-rich, silicon-graphite lithium-ion cell during fast charging. *J. Power Sources* **2019**, *412*, 204–223.
- (13) Park, G.-T.; Yoon, D. R.; Kim, U.-H.; Namkoong, B.; Lee, J.; Wang, M. M.; Lee, A. C.; Gu, X. W.; Chueh, W. C.; Yoon, C. S.; Sun, Y.-K. Ultrafine-grained ni-rich layered cathode for advanced li-ion batteries. *Energy Environ. Sci.* **2021**, *14*, 6616–6626.
- (14) Kurzhals, P.; Riewald, F.; Bianchini, M.; Sommer, H.; Gasteiger, H. A.; Janek, J. The  $\text{LiNiO}_2$  cathode active material: A comprehensive study of calcination conditions and their correlation with physicochemical properties. part i. structural chemistry. *J. Electrochem. Soc.* **2021**, *168* (11), 110518.
- (15) Phattharasupakun, N.; Cormier, M. M. E.; Liu, Y.; Geng, C.; Zsoldos, E.; Hamam, I.; Liu, A.; Johnson, M. B.; Sawangphruk, M.; Dahn, J. R. A baseline kinetic study of co-free layered  $\text{Li}_{1+x}(\text{Ni}_{0.5}\text{Mn}_{0.5})_{1-x}\text{O}_2$  positive electrode materials for lithium-ion batteries. *J. Electrochem. Soc.* **2021**, *168* (11), 110502.
- (16) Ren, D.; Padgett, E.; Yang, Y.; Shen, L.; Shen, Y.; Levin, B. D. A.; Yu, Y.; DiSalvo, F. J.; Muller, D. A.; Abruna, H. D. Ultrahigh rate performance of a robust lithium nickel manganese cobalt oxide cathode with preferentially orientated li-diffusing channels. *ACS Appl. Mater. Interfaces* **2019**, *11* (44), 41178–41187.
- (17) Yan, P.; Zheng, J.; Gu, M.; Xiao, J.; Zhang, J.-G.; Wang, C.-M. Intragranular cracking as a critical barrier for high-voltage usage of layer-structured cathode for lithium-ion batteries. *Nat. Commun.* **2017**, *8* (1), 14101.
- (18) Lin, F.; Markus, I. M.; Nordlund, D.; Weng, T.-C.; Asta, M. D.; Xin, H. L.; Doeff, M. M. Surface reconstruction and chemical evolution of stoichiometric layered cathode materials for lithium-ion batteries. *Nat. Commun.* **2014**, *5*, 3529.
- (19) Lin, F.; Nordlund, D.; Markus, I. M.; Weng, T.-C.; Xin, H. L.; Doeff, M. M. Profiling the nanoscale gradient in stoichiometric layered cathode particles for lithium-ion batteries. *Energy Environ. Sci.* **2014**, *7* (9), 3077–3085.
- (20) Xu, C.; Marker, K.; Lee, J.; Mahadevegowda, A.; Reeves, P. J.; Day, S. J.; Groh, M. F.; Emge, S. P.; Ducati, C.; Layla Mehdi, B.; Tang, C. C.; Grey, C. P. Bulk fatigue induced by surface reconstruction in layered ni-rich cathodes for li-ion batteries. *Nat. Mater.* **2021**, *20* (1), 84–92.
- (21) Yu, H.; Cao, Y.; Chen, L.; Hu, Y.; Duan, X.; Dai, S.; Li, C.; Jiang, H. Surface enrichment and diffusion enabling gradient-doping and coating of ni-rich cathode toward li-ion batteries. *Nat. Commun.* **2021**, *12* (1), 4564.
- (22) Yan, W.; Yang, S.; Huang, Y.; Yang, Y.; Yuan, G. A review on doping/coating of nickel-rich cathode materials for lithium-ion batteries. *J. Alloys Compd.* **2020**, *819*, 153048.
- (23) Zachman, M. J.; Tu, Z.; Choudhury, S.; Archer, L. A.; Kourkoutis, L. F. Cryo-stem mapping of solid–liquid interfaces and dendrites in lithium-metal batteries. *Nature* **2018**, *560* (7718), 345–349.
- (24) Sui, T.; Song, B.; Dluhos, J.; Lu, L.; Korsunsky, A. M. Nanoscale chemical mapping of li-ion battery cathode material by fibsem and tof-sims multi-modal microscopy. *Nano Energy* **2015**, *17*, 254–260.
- (25) McClary, S. A.; Long, D. M.; Sanz-Matias, A.; Kotula, P. G.; Prendergast, D.; Jungjohann, K. L.; Zavadil, K. R. A heterogeneous oxide enables reversible calcium electrodeposition for a calcium battery. *ACS Energy Lett.* **2022**, *7*, 2792–2800.
- (26) Cooper, S. J.; Roberts, S. A.; Liu, Z.; Winiarski, B. I. Methods—Kintsugi imaging of battery electrodes: Distinguishing pores from the carbon binder domain using PT deposition. *J. Electrochem. Soc.* **2022**, *169* (7), 070512.
- (27) Quinn, A.; Moutinho, H.; Usseglio-Viretta, F.; Verma, A.; Smith, K.; Keyser, M.; Finegan, D. P. Electron backscatter diffraction for investigating lithium-ion electrode particle architectures. *Cell Reports Physical Science* **2020**, *1* (8), 100137.
- (28) Devaraj, A.; Gu, M.; Colby, R.; Yan, P.; Wang, C. M.; Zheng, J. M.; Xiao, J.; Genc, A.; Zhang, J. G.; Belharouak, I.; Wang, D.; Amine, K.; Thevuthasan, S. Visualizing nanoscale 3d compositional fluctuation of lithium in advanced lithium-ion battery cathodes. *Nat. Commun.* **2015**, *6* (1), 8014.
- (29) Kim, S.-H.; Antonov, S.; Zhou, X.; Stephenson, L. T.; Jung, C.; El-Zoka, A. A.; Schreiber, D. K.; Conroy, M.; Gault, B. Atom probe analysis of electrode materials for li-ion batteries: challenges and ways forward. *Journal of Materials Chemistry A* **2022**, *10*, 4926–4935.
- (30) Stetson, C.; Yoon, T.; Coyle, J.; Nemeth, W.; Young, M.; Norman, A.; Pylypenko, S.; Ban, C.; Jiang, C.-S.; Al-Jassim, M.; Burrell, A. Three-dimensional electronic resistivity mapping of solid electrolyte interphase on si anode materials. *Nano Energy* **2019**, *55*, 477–485.
- (31) Kitta, M.; Fukada, C. Scanning spreading resistance microscopy: A promising tool for probing the reaction interface of li-ion battery materials. *Langmuir* **2019**, *35* (26), 8726–8731.
- (32) Tan, C.; Leach, A. S.; Heenan, T. M. M.; Parks, H.; Jervis, R.; Weker, J. N.; Brett, D. J. L.; Shearing, P. R. Nanoscale state-of-charge heterogeneities within polycrystalline nickel-rich layered oxide cathode materials. *Cell Reports Physical Science* **2021**, *2* (12), 100647.
- (33) Finegan, D. P.; Scheel, M.; Robinson, J. B.; Tjaden, B.; Di Michiel, M.; Hinds, G.; Brett, D. J. L.; Shearing, P. R. Investigating lithium-ion battery materials during overcharge-induced thermal runaway: an operando and multi-scale x-ray ct study. *Phys. Chem. Chem. Phys.* **2016**, *18*, 30912–30919.
- (34) Furat, O.; Finegan, D. P.; Diercks, D.; Usseglio-Viretta, F.; Smith, K.; Schmidt, V. Mapping the architecture of single electrode particles in 3d, using electron backscatter diffraction and machine learning segmentation. *J. Power Sources* **2021**, *483*, 229148.
- (35) McDonald, S. A.; Holzner, C.; Lauridsen, E. M.; Reischig, P.; Merkle, A. P.; Withers, P. J. Microstructural evolution during sintering of copper particles studied by laboratory diffraction contrast tomography (labdct). *Sci. Rep.* **2017**, *7* (1), 5251.
- (36) Jungjohann, K. L.; Gannon, R. N.; Goriparti, S.; Randolph, S. J.; Merrill, L. C.; Johnson, D. C.; Zavadil, K. R.; Harris, S. J.; Harrison, K. L. Cryogenic laser ablation reveals short-circuit mechanism in lithium metal batteries. *ACS Energy Letters* **2021**, *6* (6), 2138–2144.
- (37) Robertson, I. M.; Schuh, C. A.; Vetrano, J. S.; Browning, N. D.; Field, D. P.; Jensen, D. J.; Miller, M. K.; Baker, I.; Dunand, D. C.; Dunin-Borkowski, R.; et al. Towards an integrated materials characterization toolbox. *J. Mater. Res.* **2011**, *26* (11), 1341–1383.
- (38) Furat, O.; Petrich, L.; Finegan, D. P.; Diercks, D.; Usseglio-Viretta, F.; Smith, K.; Schmidt, V. Artificial generation of representative single li-ion electrode particle architectures from microscopy data. *npj Computational Materials* **2021**, *7* (1), 105.
- (39) Xu, H.; Usseglio-Viretta, F.; Kench, S.; Cooper, S. J.; Finegan, D. P. Microstructure reconstruction of battery polymer separators by fusing 2d and 3d image data for transport property analysis. *J. Power Sources* **2020**, *480*, 229101.
- (40) Dahari, A.; Kench, S.; Squires, I.; Cooper, S. J. Super-resolution of multiphase materials by combining complementary 2d and 3d image data using generative adversarial networks. *arXiv Preprint* **2021**, arXiv:2110.11281v2.
- (41) Gayon-Lombardo, A.; Mosser, L.; Brandon, N. P.; Cooper, S. J. Pores for thought: generative adversarial networks for stochastic

reconstruction of 3d multi-phase electrode microstructures with periodic boundaries. *npj Computational Materials* **2020**, *6* (82), 82.

(42) Squires, I.; Cooper, S. J.; Dahari, A.; Kench, S. Two approaches to inpainting microstructure with deep convolutional generative adversarial networks. *arXiv Preprint* **2022**, arXiv:2210.06997.

(43) Furat, O.; Finegan, D. P.; Yang, Z.; Kirstein, T.; Smith, K.; Schmidt, V. Super-resolving microscopy images of li-ion electrodes for fine-feature quantification using generative adversarial networks. *npj Computational Materials* **2022**, *8* (1), 1–11.

(44) Kench, S.; Cooper, S. J. Generating three-dimensional structures from a two-dimensional slice with generative adversarial network-based dimensionality expansion. *Nature Machine Intelligence* **2021**, *3*, 299–305.

(45) Spurgeon, S. R.; Ophus, C.; Jones, L.; Petford-Long, A.; Kalinin, S. V.; Olszta, M. J.; Dunin-Borkowski, R. E.; Salmon, N.; Hattar, K.; Yang, W.-C. D.; et al. Towards data-driven next-generation transmission electron microscopy. *Nature materials* **2021**, *20* (3), 274–279.

(46) Borodinov, N.; Tsai, W.-Y.; Korolkov, V. V.; Balke, N.; Kalinin, S. V.; Ovchinnikova, O. S. Machine learning-based multidomain processing for texture-based image segmentation and analysis. *Appl. Phys. Lett.* **2020**, *116* (4), 044103.

(47) Akers, S.; Kautz, E.; Trevino-Gavito, A.; Olszta, M.; Matthews, B. E.; Wang, L.; Du, Y.; Spurgeon, S. R. Rapid and flexible segmentation of electron microscopy data using few-shot machine learning. *npj Computational Materials* **2021**, *7* (1), 187.

(48) Ronneberger, O.; Fischer, P.; Brox, T. U-net: Convolutional networks for biomedical image segmentation. *International Conference on Medical image computing and computer-assisted intervention*; Springer, 2015; pp 234–241.

(49) Arganda-Carreras, I.; Kaynig, V.; Rueden, C.; Eliceiri, K. W.; Schindelin, J.; Cardona, A.; Seung, H. S. Trainable weka segmentation: a machine learning tool for microscopy pixel classification. *Bioinformatics* **2017**, *33*, 2424–2426.

(50) Gatys, L. A.; Ecker, A. S.; Bethge, M. Image style transfer using convolutional neural networks. *Proceedings of the IEEE Conference on Computer Vision and Pattern Recognition*; IEEE, 2016; pp 2414–2423.

(51) Yu, J.; Lin, Z.; Yang, J.; Shen, X.; Lu, X.; Huang, T. S. Generative image inpainting with contextual attention. *Proceedings of the IEEE Conference on Computer Vision and Pattern Recognition*; IEEE, 2018; pp 5505–5514.

(52) Liu, Y.; Caselles, V. Exemplar-based image inpainting using multiscale graph cuts. *IEEE Trans. Image Process.* **2013**, *22* (5), 1699–1711.

(53) MA, B.; MA, B.; GAO, M.; WANG, Z.; BAN, X.; HUANG, H.; WU, W. Deep learning-based automatic inpainting for material microscopic images. *J. Microsc.* **2021**, *281* (3), 177–189.

(54) Karamov, R.; Lomov, S. V.; Sergeichev, I.; Swolfs, Y.; Akhatov, I. Inpainting micro-CT images of fibrous materials using deep learning. *Comput. Mater. Sci.* **2021**, *197*, 110551.

(55) Nicholls, D.; Lee, J.; Amari, H.; Stevens, A. J.; Mehdi, B. L.; Browning, N. D. Minimising damage in high resolution scanning transmission electron microscope images of nanoscale structures and processes. *Nanoscale* **2020**, *12* (41), 21248–21254.

(56) Goodfellow, I.; Pouget-Abadie, J.; Mirza, M.; Xu, B.; Warde-Farley, D.; Ozair, S.; Courville, A.; Bengio, Y. Generative adversarial nets. *Advances in neural information processing systems* **2014**, *27*, 139.

(57) Ho, J.; Jain, A.; Abbeel, P. Denoising diffusion probabilistic models. *34th Conference on Neural Information Processing Systems (NeurIPS 2020)*, Vancouver, Canada, 2020.

(58) Karras, T.; Laine, S.; Aila, T. A Style-Based generator architecture for generative adversarial networks. *arXiv Preprint* **2018**, arXiv:1812.04948.

(59) Rombach, R.; Blattmann, A.; Lorenz, D.; Esser, P.; Ommer, B. High-Resolution image synthesis with latent diffusion models. *arXiv Preprint* **2021**, arXiv:2112.10752.

(60) Ledig, C.; Theis, L.; Huszar, F.; Caballero, J.; Cunningham, A.; Acosta, A.; Aitken, A.; Tejani, A.; Totz, J.; Wang, Z.; et al. Photo-realistic single image super-resolution using a generative adversarial

network. *Proceedings of the IEEE Conference on Computer Vision and Pattern Recognition*, IEEE, 2017; pp 4681–4690.

(61) Fan, D.; Fang, S.; Wang, G.; Gao, S.; Liu, X. The visual human face super-resolution reconstruction algorithm based on improved deep residual network. *EURASIP J. Adv. Signal Processing* **2019**, 2019, 2019.

(62) Gui, J.; Sun, Z.; Wen, Y.; Tao, D.; Ye, J. A review on generative adversarial networks: Algorithms, theory, and applications. *IEEE Trans. Knowl. Data Eng.* **2022**, 1.

(63) Kench, S.; Squires, I.; Dahari, A.; Cooper, S. J. Microlib: A library of 3d microstructures generated from 2d micrographs using sliceGAN. *arXiv Preprint* **2022**, arXiv:2210.06541.

(64) Doyle, M.; Fuller, T. F.; Newman, J. Modeling of galvanostatic charge and discharge of the Lithium/Polymer/Insertion cell. *J. Electrochem. Soc.* **1993**, *140* (6), 1526–1533.

(65) Ngandjong, A. C.; Lombardo, T.; Primo, E. N.; Chouchane, M.; Shodiev, A.; Arcelus, O.; Franco, A. A. Investigating electrode calendaring and its impact on electrochemical performance by means of a new discrete element method model: Towards a digital twin of li-ion battery manufacturing. *J. Power Sources* **2021**, *485*, 229320.

(66) Aykol, M.; Gopal, C. B.; Anapolsky, A.; Herring, P. K.; van Vlijmen, B.; Berliner, M. D.; Bazant, M. Z.; Braatz, R. D.; Chueh, W. C.; Storey, B. D. Perspective—Combining physics and machine learning to predict battery lifetime. *J. Electrochem. Soc.* **2021**, *168* (3), 030525.

(67) Mirza, M.; Osindero, S. Conditional generative adversarial nets. *arXiv Preprint* **2014**, arXiv:1411.1784.

(68) Cooper, S.J.; Bertei, A.; Shearing, P.R.; Kilner, J.A.; Brandon, N.P. Taufactor: An open-source application for calculating tortuosity factors from tomographic data. *SoftwareX* **2016**, *5*, 203–210.

(69) Zannotto, F. M.; Zapata Dominguez, D.; Ayerbe, E.; Boyano, I.; Burmeister, C.; Duquesnoy, M.; Eisentraeger, M.; Florez Montañó, J.; Gallo-Bueno, A.; Gold, L. Data specifications for battery manufacturing digitalization: Current status, challenges, and opportunities. *Batteries Supercaps* **2022**, *5* (9), e202200224.

## Recommended by ACS

### Mesoscale Machine Learning Analytics for Electrode Property Estimation

Venkatesh Kabra, Partha P. Mukherjee, et al.

AUGUST 22, 2022  
THE JOURNAL OF PHYSICAL CHEMISTRY C

READ 

### Perspective on Mechanistic Modeling of Li-Ion Batteries

Matthieu Dubarry and David Beck

JUNE 29, 2022  
ACCOUNTS OF MATERIALS RESEARCH

READ 

### Automatically Capturing Key Features for Predicting Superionic Conductivity of Solid-State Electrolytes Using a Neural Network

Zhuole Lu, Chandra Veer Singh, et al.

JUNE 23, 2022  
ACS APPLIED ENERGY MATERIALS

READ 

### Evaluation of Various Offline and Online ECM Parameter Identification Methods of Lithium-Ion Batteries in Underwater Vehicles

Peiyu Chen, Yunwei Xu, et al.

AUGUST 19, 2022  
ACS OMEGA

READ 

Get More Suggestions >